

Electronic Supplementary Information (ESI).

## Vortex fluidic mediated synthesis of polysulfone

Aghil Igder<sup>a,b</sup>, Scott J. Pye<sup>b</sup>, Ahmed Hussein Mohammed Al-Antaki<sup>b</sup>, Alireza Keshavarz<sup>a</sup>, and Colin L. Raston<sup>\*b</sup>, Ata Nosrati<sup>a</sup>

<sup>a</sup> School of Engineering, Edith Cowan University, Joondalup, Perth, WA 6027, Australia.

<sup>b</sup> Flinders Institute for Nanoscale Science and Technology, College of Science and Engineering, Flinders University, Adelaide, SA 5042, Australia.  
E-mail: [colin.raston@flinders.edu.au](mailto:colin.raston@flinders.edu.au).

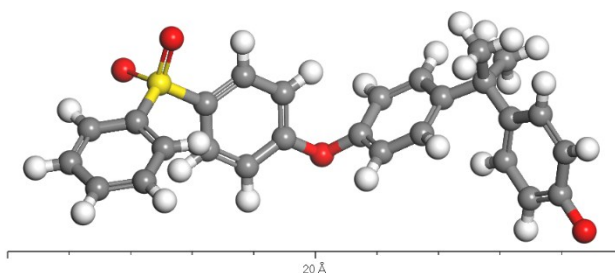
### Contents

<b>Schematic structure of Polysulfone (PSF) .....</b>	<b>3</b>
PSF repeating unit .....	3
Polysulfone (PSF) with a number of repeating units.....	3
<b>PSF polymerization via conventional technique .....</b>	<b>3</b>
<b>Experimental setup for PSF polymerization via the VFD .....</b>	<b>4</b>
<b>FTIR spectra .....</b>	<b>6</b>
BPA & DiNa salt of BPA .....	6
Polysulfone (PSF).....	7
<b>NMR spectra .....</b>	<b>7</b>
Bisphenol A (BPA).....	7
Disodium salt of BPA .....	8
4,4-dichlorodiphenyl sulphone (DCDPS) .....	9
Polysulfone (PSF).....	9
<b>GPC curves .....</b>	<b>10</b>
GPC traces of VFD ( $T_4$ , 6000 rpm), commercial and conventional PSF .....	11
Effect of rotational speed .....	12
Effect of temperature .....	13
GPC traces of VFD ( $T_{11}$ , 160 °C), commercial and conventional PSF .....	14
Effect of tilt angle .....	15
Effect of time.....	16
GPC traces on the VFD synthesized PSFs ( $T_1 - T_{22}$ ), conventional and commercial PSFs. ....	17

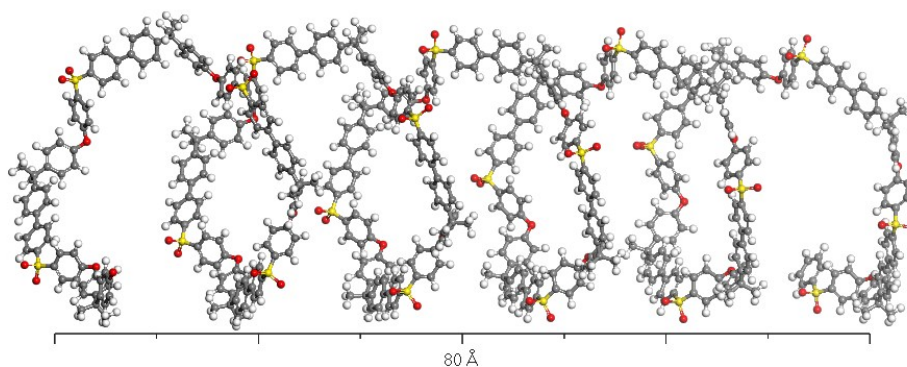
<b>Glass transition temperature (<math>T_g</math>)</b> .....	<b>17</b>
Comparison between $T_g$ obtained for commercial PSF and VFD prepared PSF in different $\omega$ .....	18
<b>TGA</b> .....	<b>18</b>
<b>SEM images</b> .....	<b>19</b>
<b>References</b> .....	<b>20</b>

## Schematic structure of Polysulfone (PSF)

### PSF repeating unit



### Polysulfone (PSF) with a number of repeating units



### PSF polymerization via conventional technique

Bisphenol A (6.42 g, 0.028 mol) accompanied with DMSO (13.07 mL) and chlorobenzene (37.16 mL) were placed in a triple neck rounded bottom flask. This flask was fitted with a nitrogen inlet, mechanical stirrer, and a condenser. Dissolving BPA in the solvents were performed at 60-80 °C using an overhead mechanical stirrer with 500 rpm rotational speed in 30 min resulted in a clear solution. Following this, 50% NaOH solution (4.48 g, 2.92 mL, 0.056 mol) was added to the reaction mixture over a period of 10 minutes, and the reaction was continued for 1 h at 120 °C. This resulted in a two-phase mixture of chlorobenzene, and DiNa salt of BPA in DMSO. For water removal, the temperature was increased to 140 °C, resulting in precipitation of the disodium salt of BPA.

A 50 % w/w solution of DCDPS (8.07 g, 0.028 mol), in chlorobenzene (7.27 mL) was heated to 110 °C, then added to the reaction over a period of about 10 min. The solution was then stirred at 1000 rpm for 1 h at 160 °C.<sup>1</sup> The obtained solution was cooled and diluted with chlorobenzene (90 mL). The solid NaCl was then filtered from the solution. The final polymer was coagulated in ethanol (300 mL) and washed with ethanol 3 times and filtered from the

coagulant followed by drying in an oven at 135 °C for 5 hours, resulting in pure PSF as a goldish solid.<sup>2</sup>

### Experimental setup for PSF polymerization via the VFD

*Table S 1. List of experiments conditions for optimizing the PSF polymerisation using the VFD in confined mod.*

Test No	Speed (RPM)	T (°C)	Tilt Angle (°)	Time (min)
T1	3000	150	45	30
T2	4000	150	45	30
T3	5000	150	45	30
T4	6000	150	45	30
T5	7000	150	45	30
T6	8000	150	45	30
T7	Optimal	80	45	30
T8	Optimal	120	45	30
T9	Optimal	140	45	30
T10	Optimal	150	45	30
T11	Optimal	160	45	30
T12	Optimal	170	45	30
T13	Optimal	Optimal	0	30
T14	Optimal	Optimal	15	15
T15	Optimal	Optimal	30	30
T16	Optimal	Optimal	45	60
T17	Optimal	Optimal	60	30
T18	Optimal	Optimal	75	30
T19	Optimal	Optimal	90	30
T20	Optimal	Optimal	Optimal	15
T21	Optimal	Optimal	Optimal	30
T22	Optimal	Optimal	Optimal	60

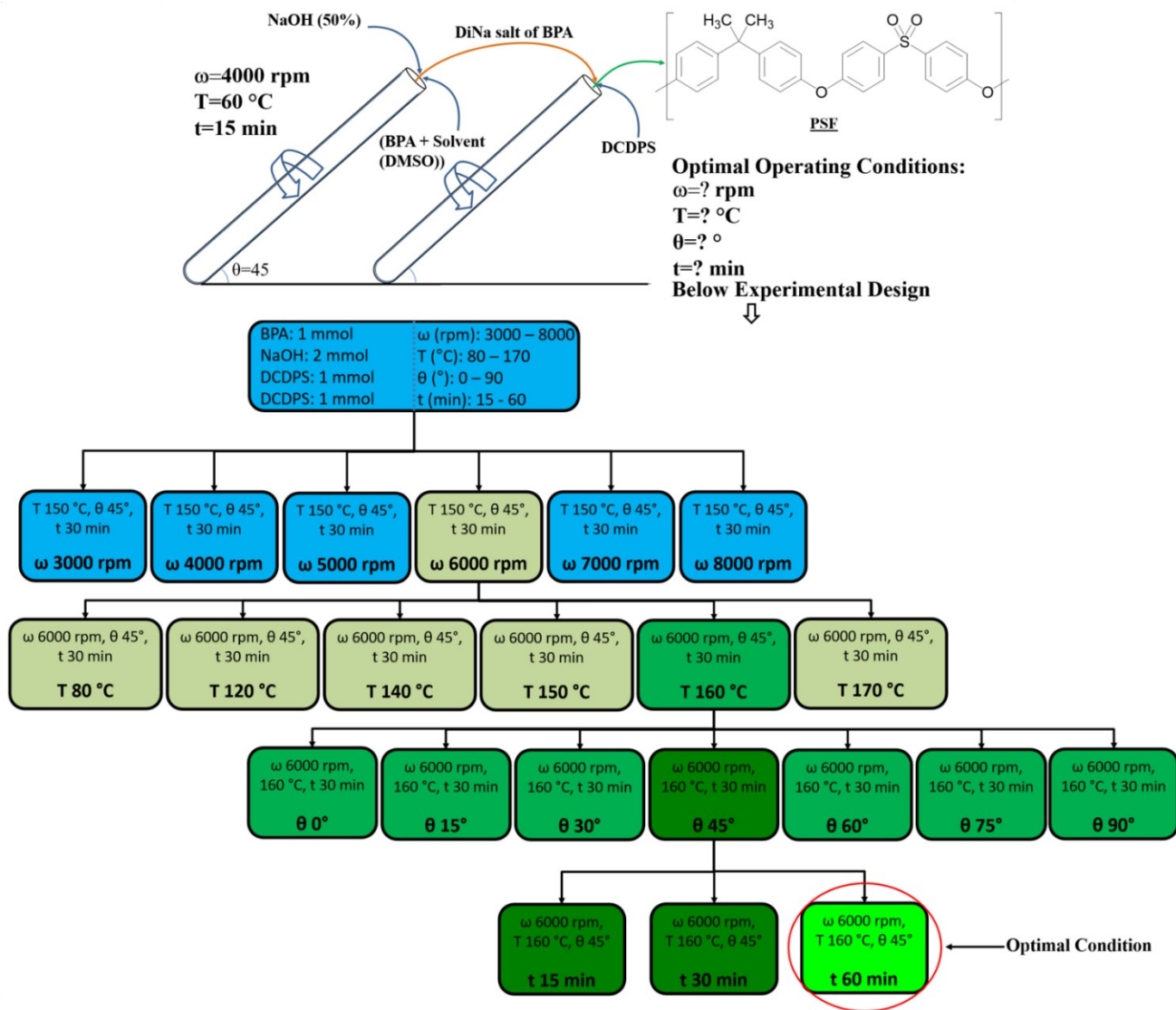


Figure S 1. Experimental setup for investigating the operating parameters in a systematic approach.

## FTIR spectra

### BPA & DiNa salt of BPA

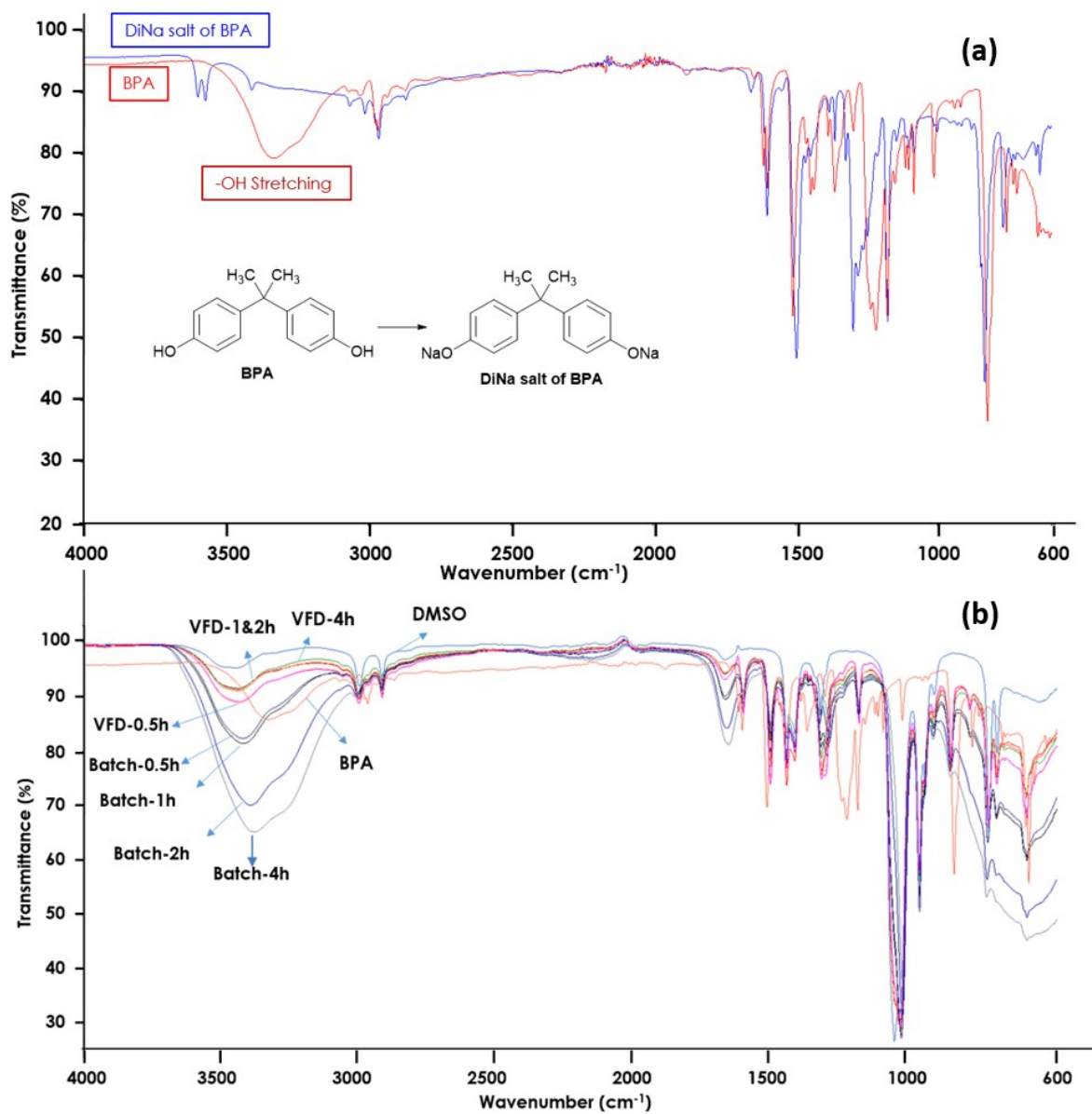


Figure S 2. FTIR spectrums of BPA and DiNa salt of BPA, b) FTIR spectrums of DiNa salt of BPA obtained from first step of polymerization in both VFD and batch processing for different retention times from 30 min to 4h in comparing the effect of time in water dissipation in producing the DiNa salt of BPA, using VFD or batch processing.

## Polysulfone (PSF)

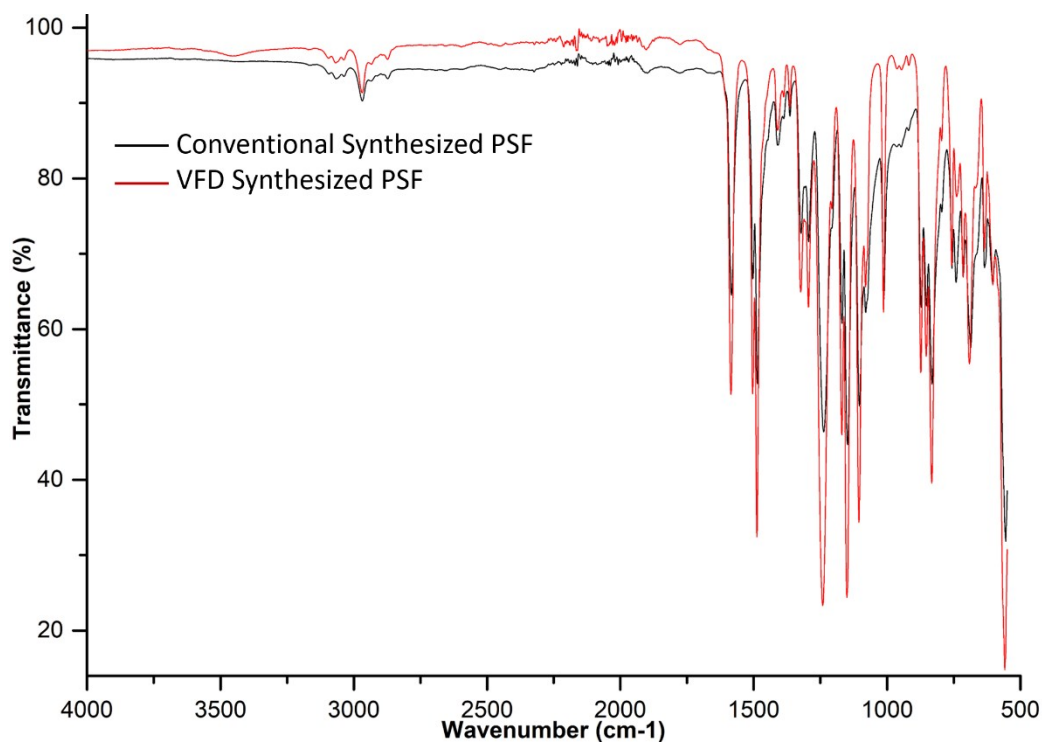


Figure S 3. FTIR spectra of the VFD and conventional synthesized PSF. VFD product was synthesised at 6000 rpm, 160 °C, 45 tilt angle, and 60 min reaction time.

## NMR spectra

All NMR was performed on either 600 or 400 MHz Bruker advance spectrometers, using CDCl<sub>3</sub> or D<sub>2</sub>O as the solvent, as specified. Spectra were acquired using a relaxation delay-time of 4 seconds. All chemical shifts are presented in ppm, using residual solvent as the internal standard. 2D COSY and HSQC experiments were used for peak allocation.

## Bisphenol A (BPA)

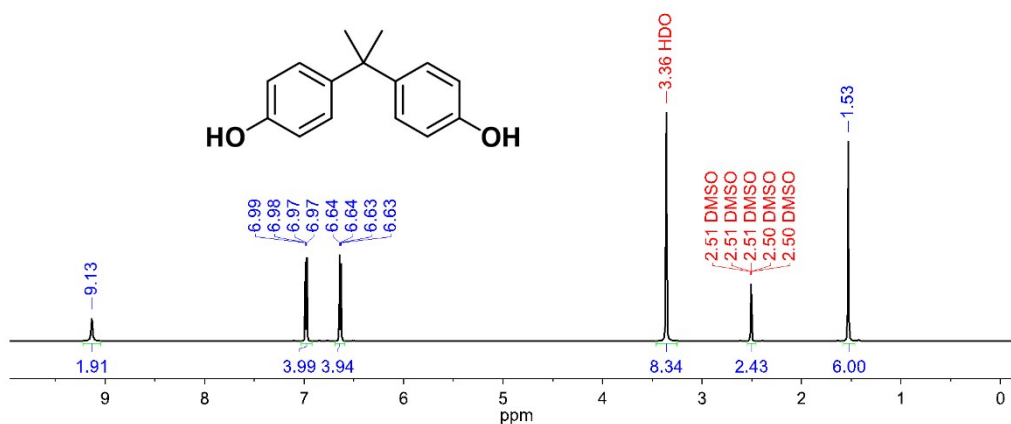


Figure S 4. <sup>1</sup>H-NMR of BPA as a starting material in first step of PSF polymerization, using DMSO-d<sub>6</sub> as the NMR solvent.

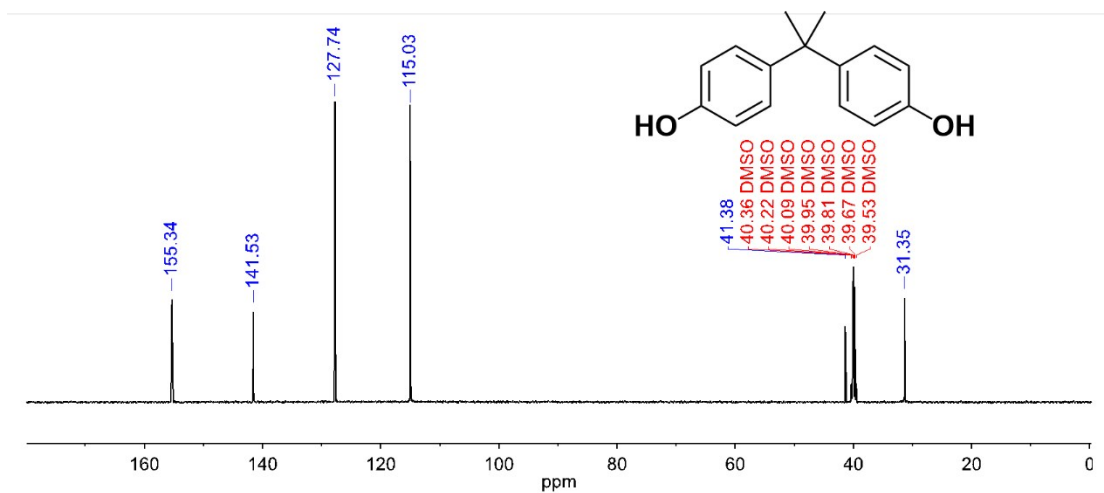


Figure S 5- <sup>13</sup>C-NMR of BPA as a starting material in first step of PSF polymerization.

Disodium salt of BPA

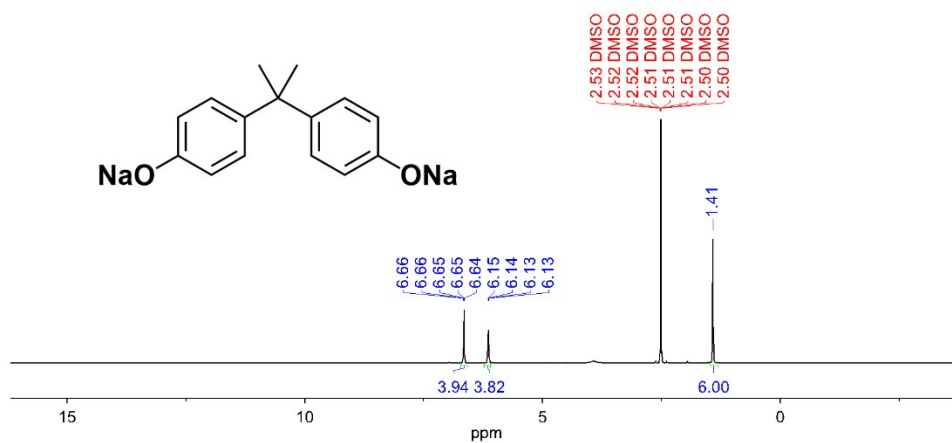


Figure S 6. <sup>1</sup>H-NMR of DiNa salt of BPA, as the intermediate product in PSF polymerization.

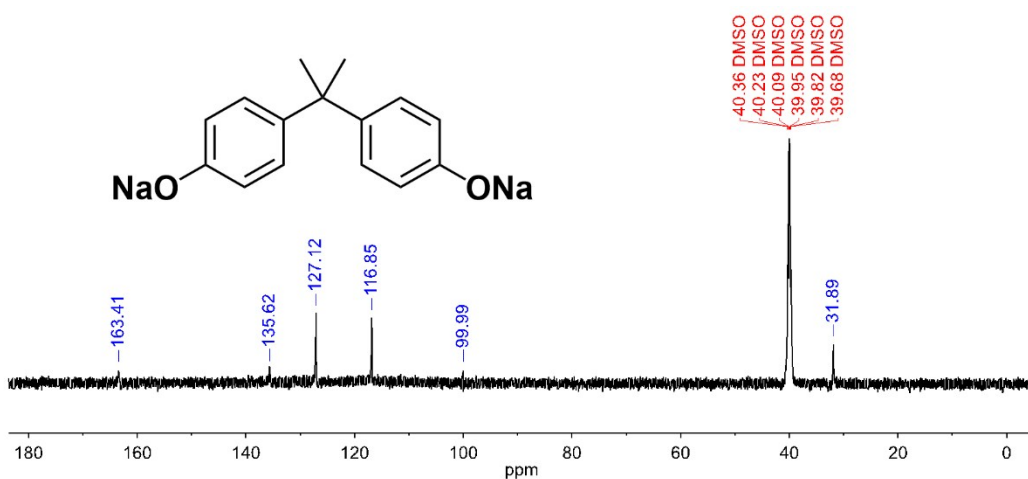


Figure S 7. <sup>13</sup>C-NMR of DiNa salt of BPA as the intermediate product in PSF polymerization.



### 4,4-dichlorodiphenyl sulphone (DCDPS)

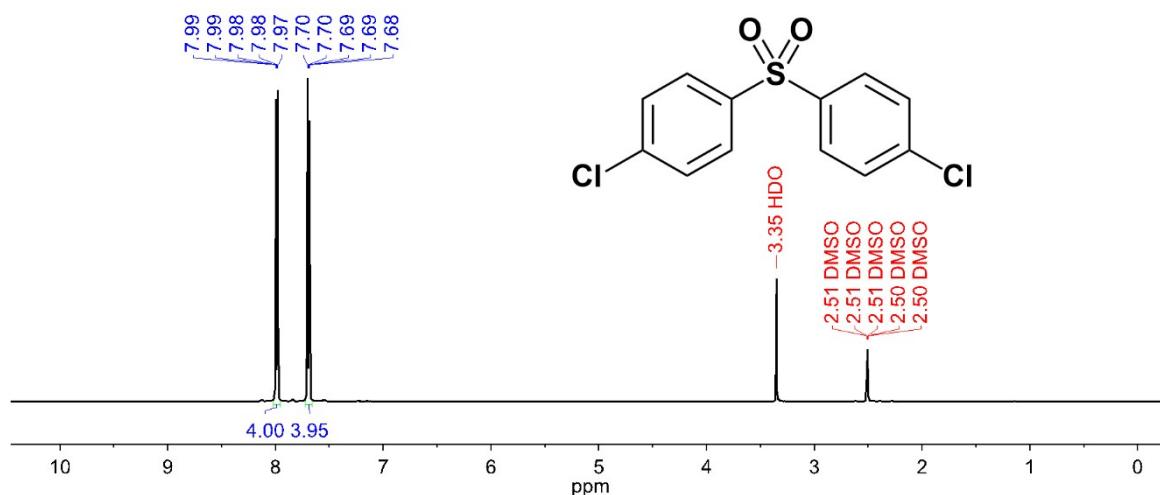


Figure S 8.  $^1\text{H-NMR}$  of DCDPS as a starting material in second step of PSF polymerization.

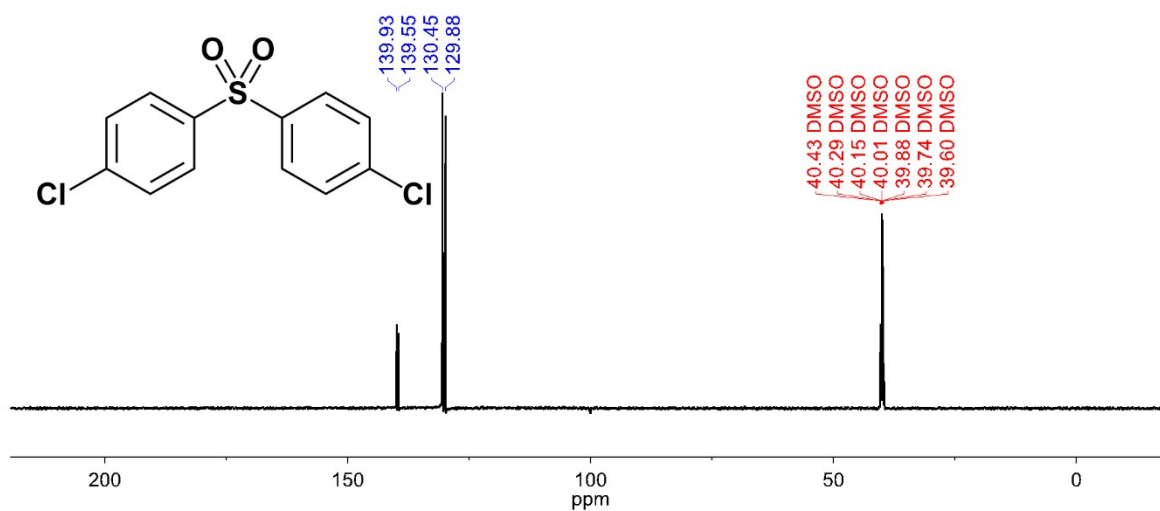


Figure S 9.  $^{13}\text{C-NMR}$  of DCDPS as a starting material in second step of PSF polymerization.

### Polysulfone (PSF)

The NMR data suggests that the reaction of BPA and DCDPS resulted in PSF. This is evident from the consumption of peaks corresponding to both starting materials, and the production of new, broadened peaks indicative of PSF. In the aromatic region, there are smaller peaks present that are likely due to terminal groups of the polymer.

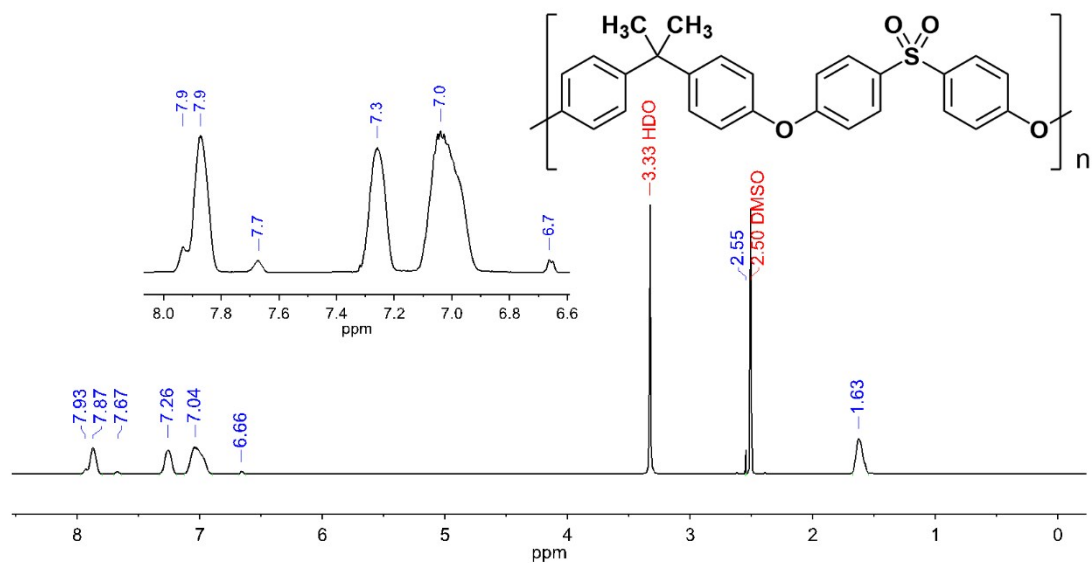


Figure S 10.  $^1\text{H-NMR}$  spectra of VFD prepared PSF at 6000 rpm, 160 °C, 45 tilt angle, and 60 min reaction time.

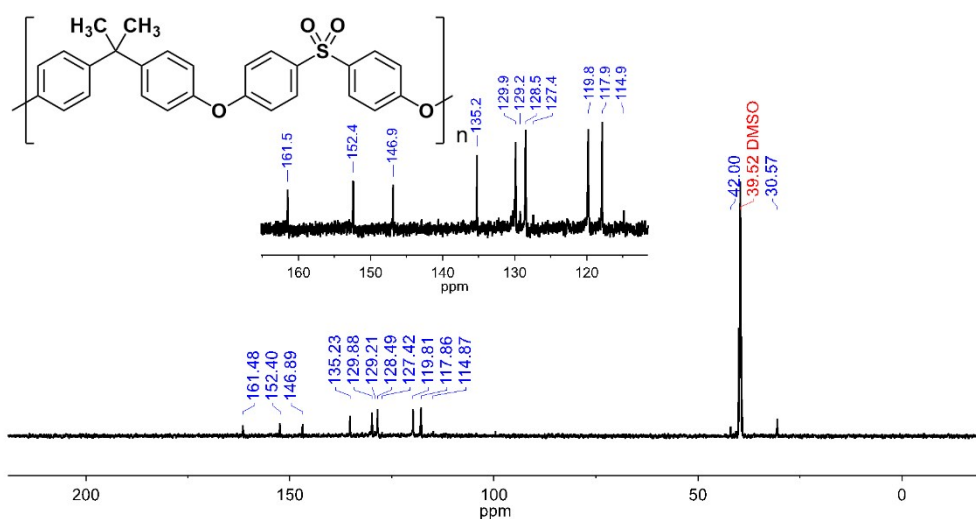


Figure S 11.  $^{13}\text{C-NMR}$  spectra of VFD prepared PSF at 6000 rpm, 160 °C, 45 tilt angle, and 60 min reaction time.

## GPC curves

Molecular weight average molar mass ( $M_w$ ) and distribution of the synthesized PSF were determined using a double detection Shimadzu GPC instrument equipped with an Ultra Violet (UV) and Refractive Index (RI) detectors, a guard column and a Phenogel™ 5 $\mu\text{m}$  Linear (2), 300 \* 7.8 mm LC column. Tetrahydrofuran (THF) was used as the eluent (at 25 °C with 1.0 ml/min flow rate). The column was calibrated using polystyrene standards with molecular weight covering the range of 1000–2704000 g/mol.

GPC traces of VFD ( $T_4$ , 6000 rpm), commercial and conventional PSF

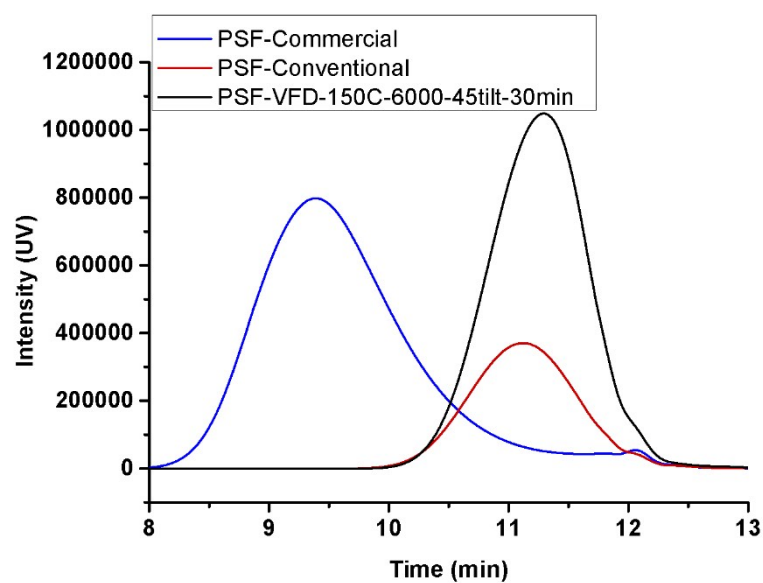


Figure S 12. Comparison between GPC traces of commercial, conventional and VFD synthesized ( $T_4$  at 6000 rpm, 150 °C, 45°, and 30 min) PSF detected using the UV detector.

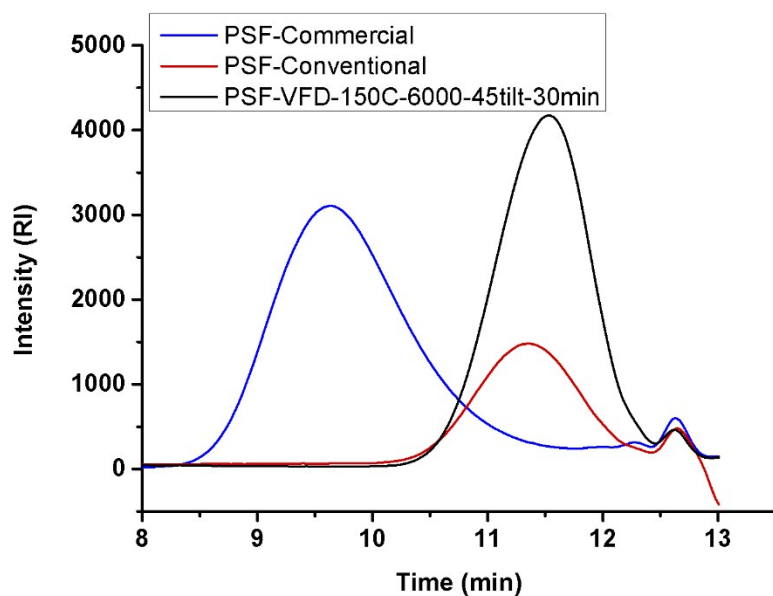


Figure S 13. Comparison between GPC traces of commercial, conventional and VFD synthesized ( $T_4$  at 6000 rpm, 150 °C, 45°, and 30 min) PSF detected using the RI detector.

## Effect of rotational speed

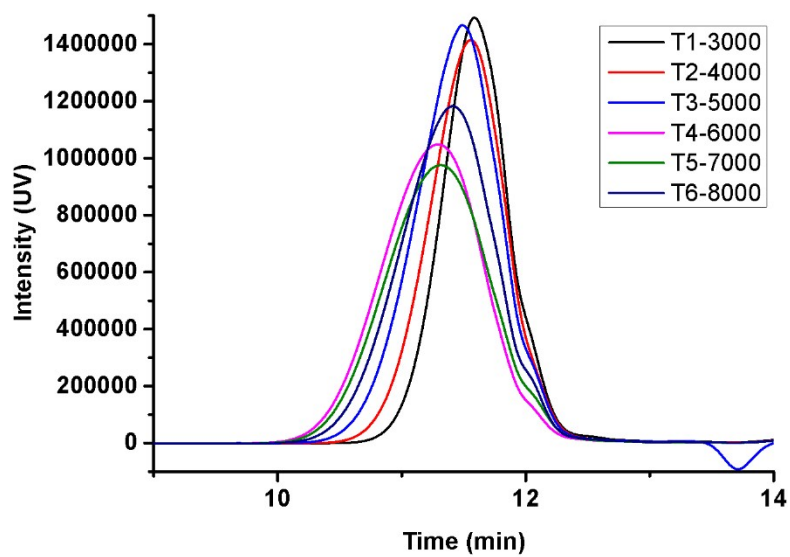


Figure S 14. GPC curves of the VFD synthesized PSF's in different rotational speed, obtained from  $T_1$  to  $T_6$  using the UV detector.

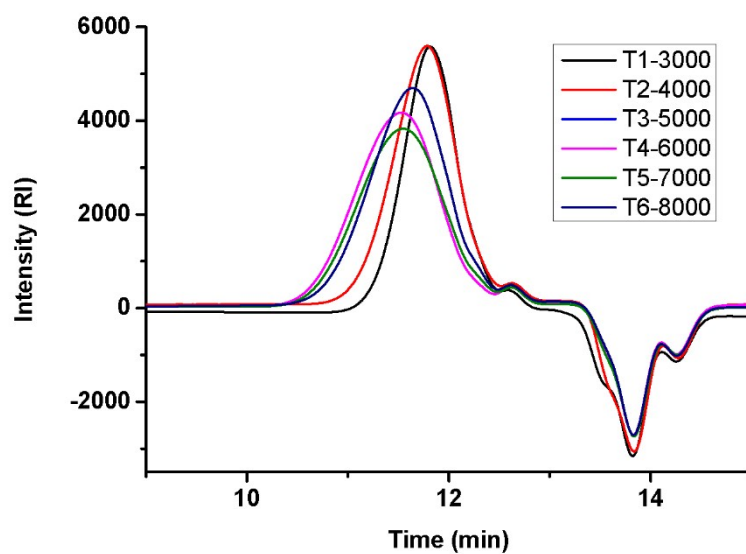


Figure S 15. GPC curves of the VFD synthesized PSF's in different rotational speed, obtained from  $T_1$  to  $T_6$  using the RI detector.

## Effect of temperature

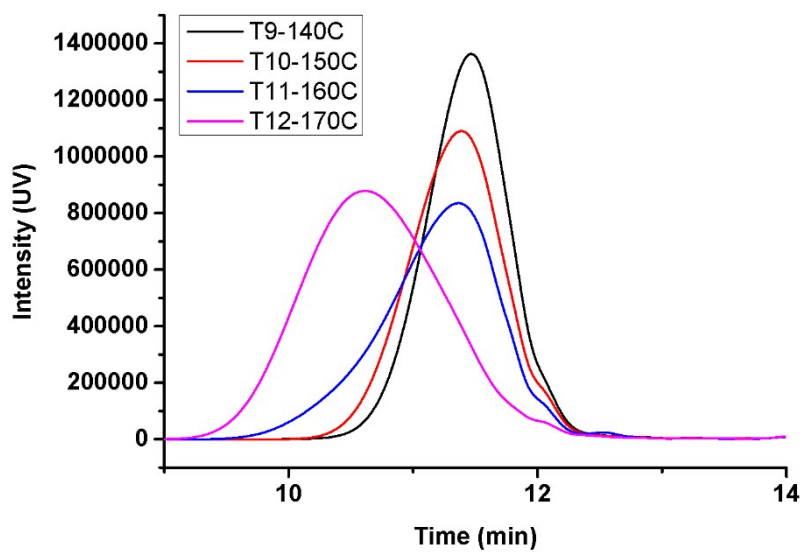


Figure S 16. GPC curves of the VFD synthesized PSF's in different temperatures, obtained from  $T_9$  to  $T_{12}$  using the UV detector.

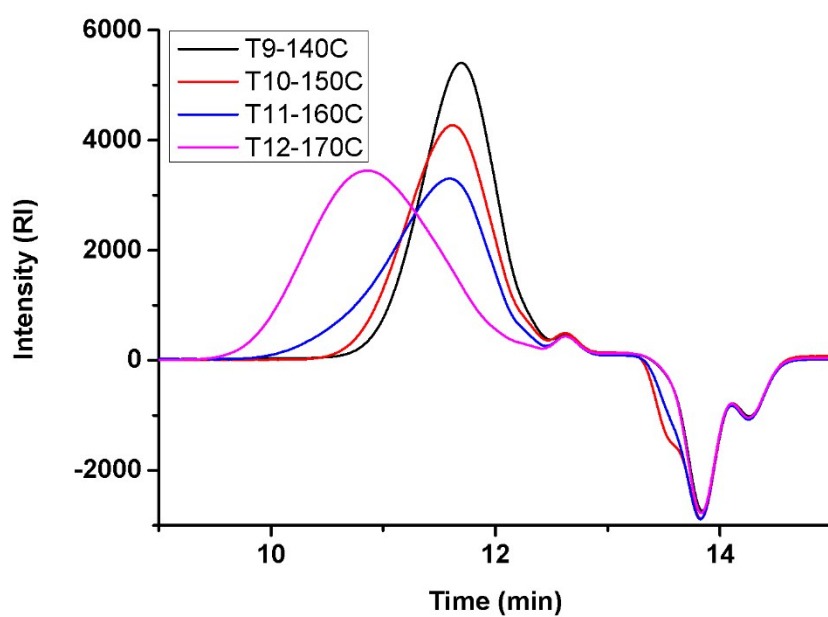


Figure S 17. GPC curves of the VFD synthesized PSF's in different temperatures, obtained from  $T_9$  to  $T_{12}$  using the RI detector.

GPC traces of VFD ( $T_{11}$ , 160 °C), commercial and conventional PSF

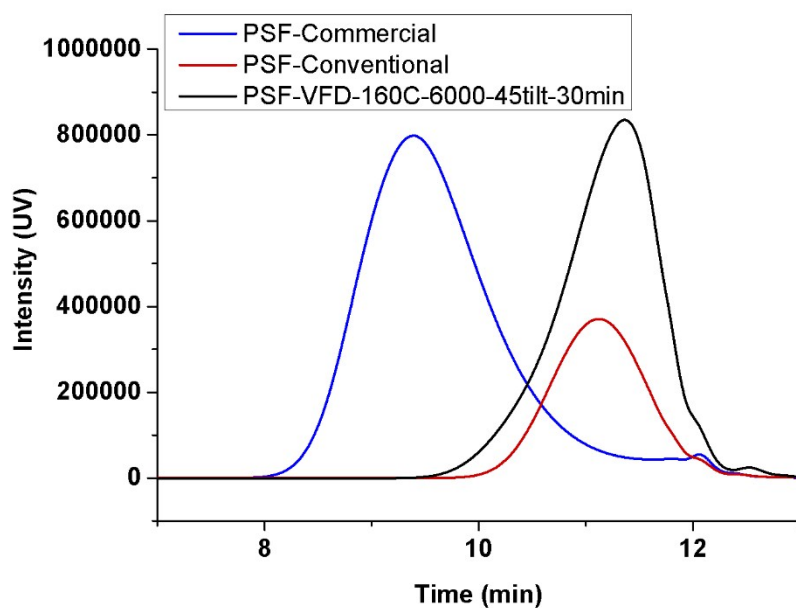


Figure S 18. Comparison between GPC traces of commercial, conventional and VFD synthesized ( $T_{11}$  at 160 °C) PSF detected using the UV detector.

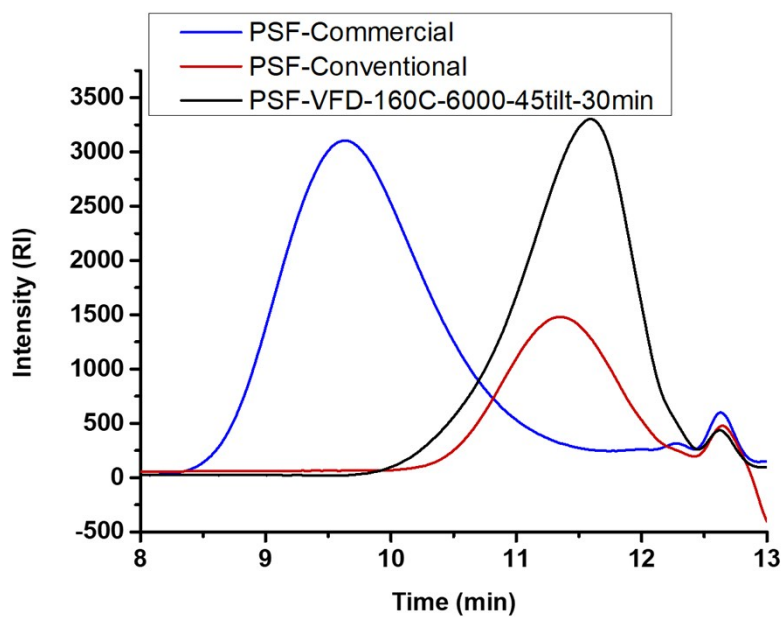


Figure S 19. Comparison between GPC traces of commercial, conventional and VFD synthesized ( $T_{11}$  at 160 °C) PSF detected using the RI detector.

## Effect of tilt angle

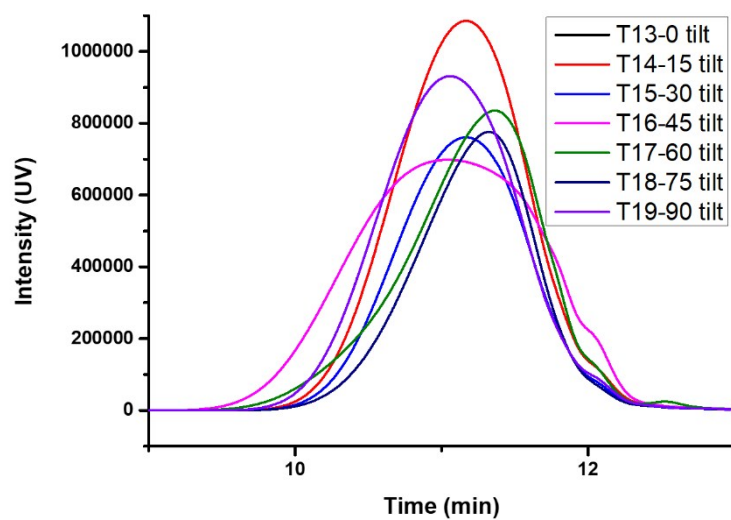


Figure S 20. GPC curves of the VFD synthesized PSF's in different tilt angles, obtained from  $T_{13}$  to  $T_{19}$  using the UV detector.

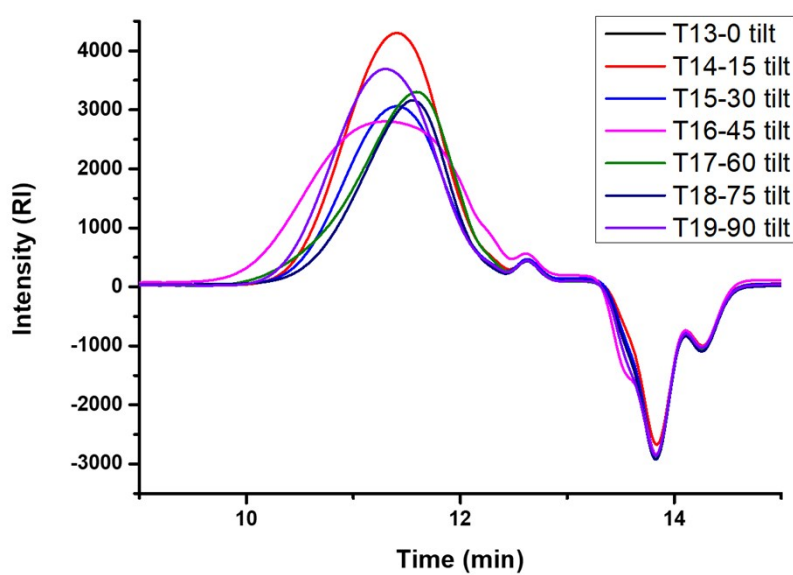


Figure S 21. GPC curves of the VFD synthesized PSF's in different tilt angles, obtained from  $T_{13}$  to  $T_{19}$  using the RI detector.

Effect of time

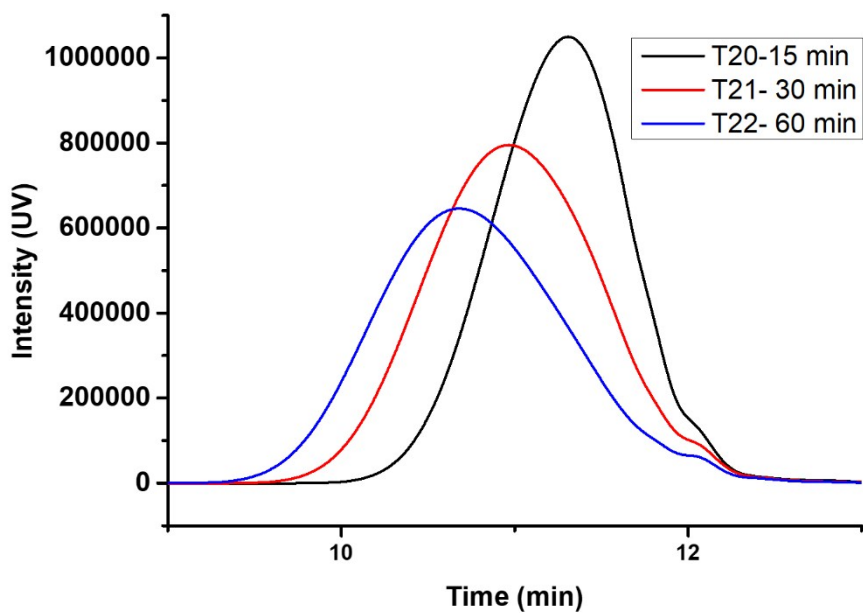


Figure S 22. GPC curves of the VFD synthesized PSF's in different retention times, obtained from  $T_{20}$  to  $T_{22}$  using the UV detector.

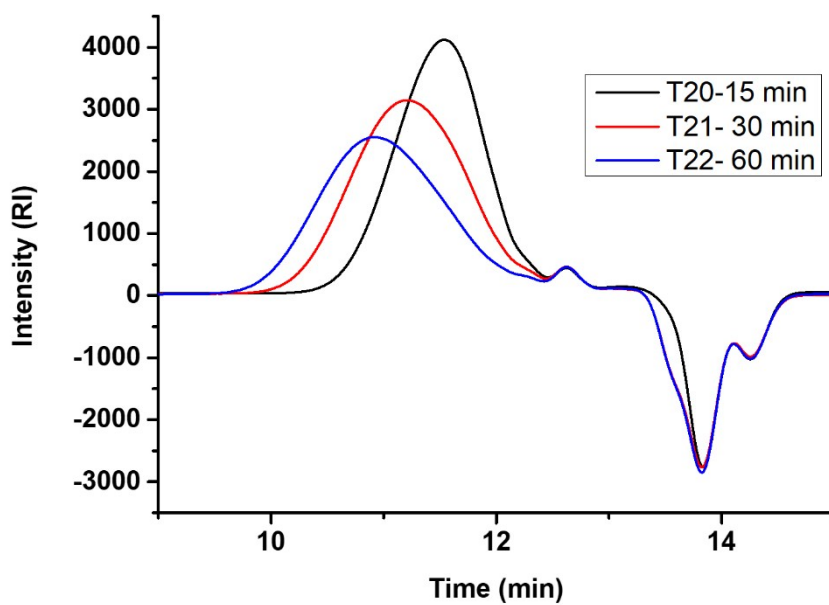


Figure S 23. GPC curves of the VFD synthesized PSF's in different retention times, obtained from  $T_{20}$  to  $T_{22}$  using the RI detector.



GPC traces on the VFD synthesized PSFs ( $T_1 - T_{22}$ ), conventional and commercial PSFs.

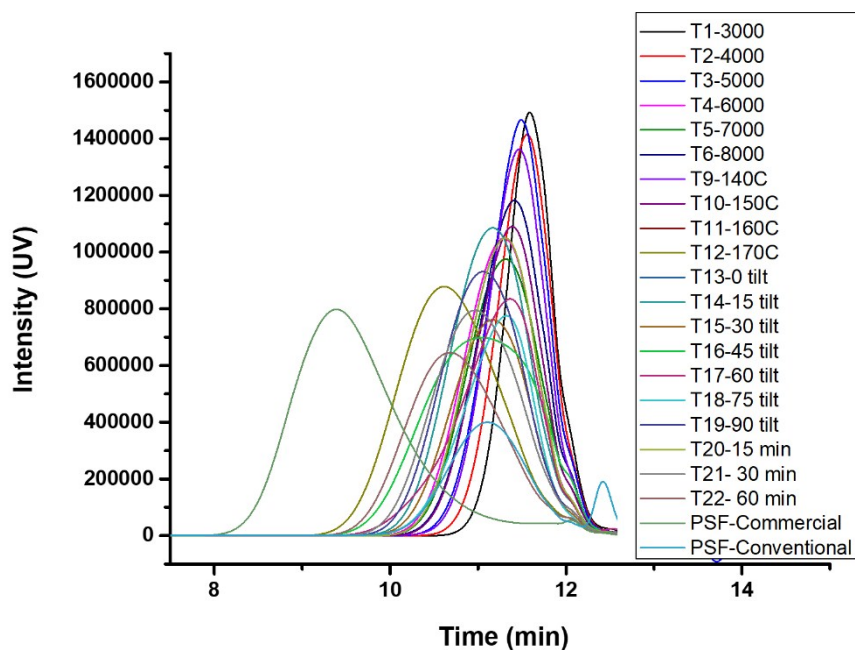


Figure S 24. GPC curves of the VFD synthesized PSF's in different operational condition, obtained from  $T_1$  to  $T_{22}$ , vs commercial and conventional PSFs, detected using the UV detector.

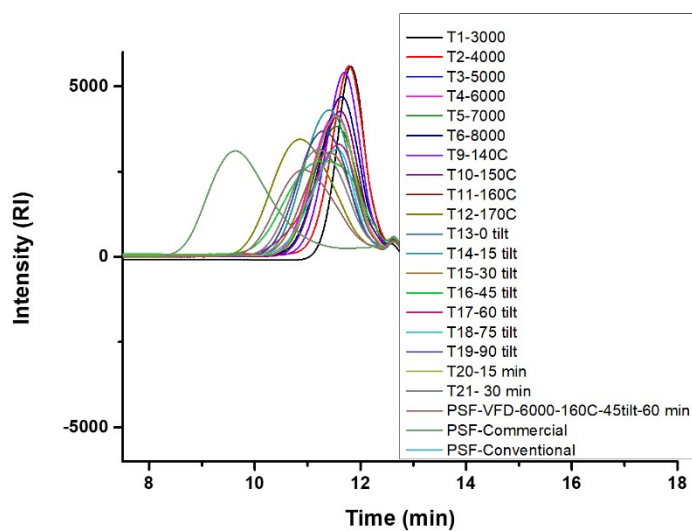


Figure S 25. GPC curves of the VFD synthesized PSF's in different operational condition, obtained from  $T_1$  to  $T_{22}$ , vs commercial and conventional PSFs, detected using the RI detector.

### Glass transition temperature ( $T_g$ )

$T_g$  measurements were proceeded using a Perkin Elmer DSC 8000 Instruments. A cyclic heating-cooling-heating was carried out to eliminate thermal history in first heating from 30 to 230°C and then cooling to 30 °C followed by heating up again to 230°C. The ramping rates

were 10 °C per minute for heating and cooling stages.  $T_g$  of each sample was obtained from the heat flow changes on the second heating scan.

Comparison between  $T_g$  obtained for commercial PSF and VFD prepared PSF in different  $\omega$

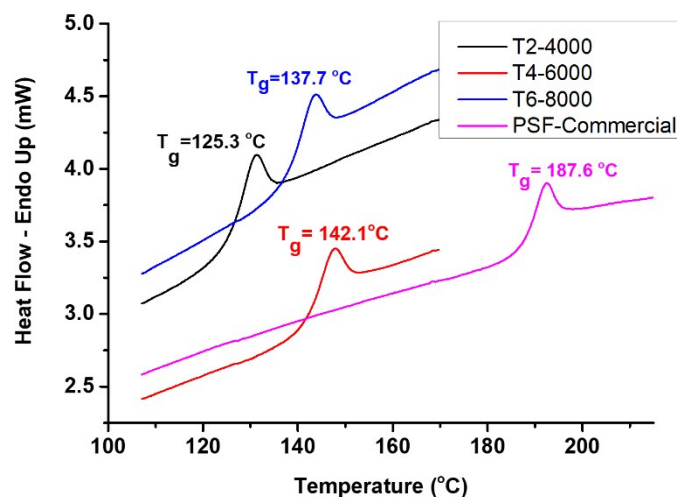


Figure S 26. DSC thermograms of commercial and VFD synthesised PSF of  $T_2$ ,  $T_4$ , and  $T_6$ . Samples were cycled from 30 °C to 230 °C at a rate of 10 °C min<sup>-1</sup>.

## TGA

TGA also is used for characterizing the thermal stabilities of materials by identifying the mass loss or gain, due to heating the samples.<sup>3</sup> Thermal stability of the polymers was also investigated through a thermogravimetric analysis on a Perkin Elmer TGA 8000 under nitrogen and air atmosphere. To do so, samples were heated up to 850 °C from 50 °C with 20 °C/min under nitrogen atmosphere and then held isothermal at 850 °C for 1 min followed by heating up again to 1050 °C with the same ramping rate under switched atmosphere to air.

Table S 2. TGA measurements settings

Sample name	Polysulfone (PSF)
Sample mass [mg]	≈ 4
Crucible	Ceramic
Temperature Program	50 ... 850 ... 1050 °C
Heating rate	20 °C / min
Atmosphere	Nitrogen, switch to air at 850 °C

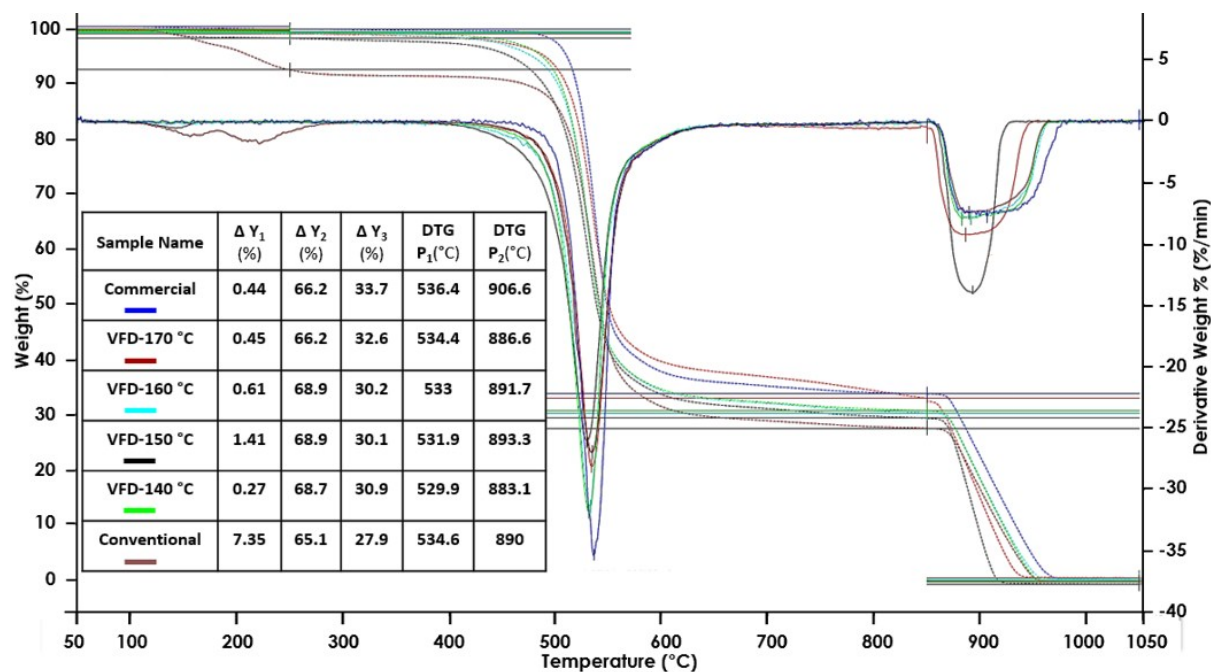


Figure S 27. TGA traces of commercial, conventional and VFD synthesized PSF ( $T_9-T_{12}$ ), heating at a rate of  $20\text{ }^\circ\text{C min}^{-1}$  up to  $850\text{ }^\circ\text{C}$  under Nitrogen and then air to  $1050\text{ }^\circ\text{C}$ .  $\Delta Y$  = Delta Y which represents the mass loose percentage in every stage. DTG  $P$  = DTG Peak represents the decomposition temperature of every mass losing step obtained from derivative weight % curve, DTG  $P_{1\&2}$  represent the decomposition temperature of main mass losing while using  $N_2$  and air, respectively.

After switching to air, burning of the pyrolytic soot as a mass loss of  $\sim 30\%$  was also observed which resulted in no residual mass at the end of the measurement.

## SEM images

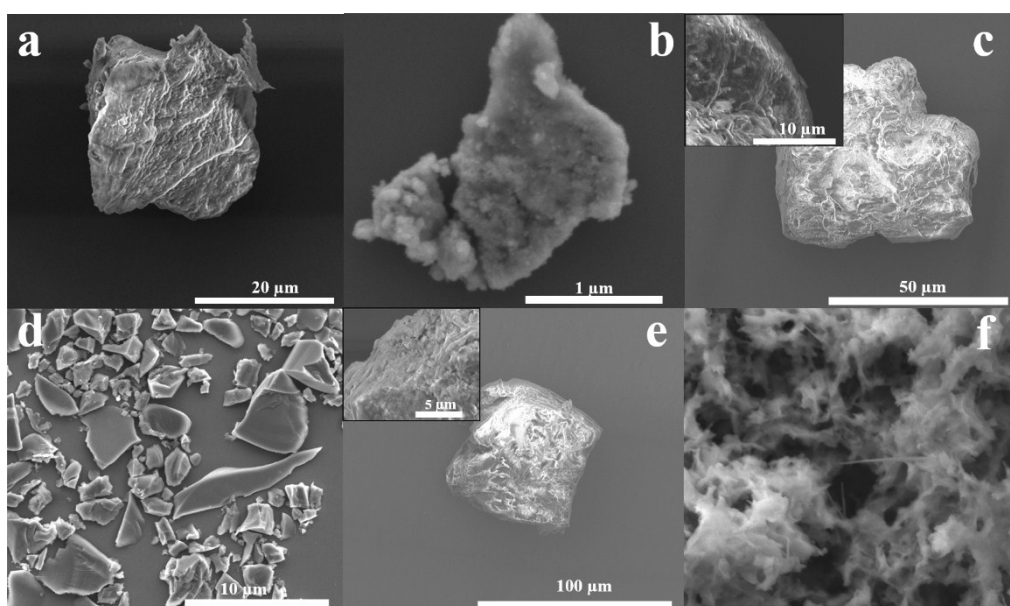


Figure S 28. SEM images of PSF for (a) commercial material, (b) material formed using conventional batch processing, (c) material formed in the VFD at the optimised  $s$  ( $T_{22}$  at  $6000\text{ rpm}$ ,  $160\text{ }^\circ\text{C}$ ,  $45^\circ$ , and  $60\text{ min}$ ). PSF synthesised in the VFD at  $6000\text{ rpm}$ ,  $160\text{ }^\circ\text{C}$ ,  $q\ 45^\circ$  for (d)  $15\text{ min}$ , (e)  $30\text{ min}$ , and (f)  $90\text{ min}$  reaction time. All the sample were drop cast and coated with ca  $5\text{ nm}$  layer of Pt.

## References

1. K. Othmer, *Encyclopedia of Chemical Technology*, Wiley, New York, 4th edn.,1996, **19**.
2. R. N. Johnson, A. G. Farnham, R. A. Clendining, W. F. Hale and C. N. Merriam, *J. Polym. Sci.: Part A-1*, 1967, **5**, 2375-2398.
3. O. Agboola, J. Maree and R. Mbaya, *Environ. Chem. Lett.*, 2014, **12**, 241-255.